Brain Stimulation 10 (2017) 65–74

Contents lists available at ScienceDirect

Brain Stimulation

journal homepage: www.brainstimjrnl.com

Investigating TMS–EEG Indices of Long-Interval Intracortical Inhibition at Different Interstimulus Intervals

George M. Opie [a,*], Nigel C. Rogasch [b], Mitchell R. Goldsworthy [c,d], Michael C. Ridding [c], John G. Semmler [a]

[a] Discipline of Physiology, School of Medicine, The University of Adelaide, Adelaide, Australia
[b] Brain and Mental Health Laboratory, School of Psychological Sciences and Monash Biomedical Imaging, Monash Institute of Cognitive and Clinical Neuroscience, Monash University, Australia
[c] Robinson Research Institute, School of Medicine, The University of Adelaide, Adelaide, Australia
[d] Discipline of Psychiatry, School of Medicine, The University of Adelaide, Adelaide, Australia

ARTICLE INFO

Article history:
Received 4 May 2016
Received in revised form 2 August 2016
Accepted 6 August 2016
Available online 8 August 2016

Keywords:
Transcranial magnetic stimulation
Electroencephalography
Long-interval intracortical inhibition
Interstimulus interval
TMS-evoked potential
GABA

ABSTRACT

Background: Long-interval intracortical inhibition (LICI) is a transcranial magnetic stimulation (TMS) paradigm that uses paired magnetic stimuli separated by 100–200 ms to investigate the activity of cortical GABAergic interneurons. While commonly applied, the mechanisms contributing to LICI are not well understood, and growing evidence suggests that inhibition observed at different interstimulus intervals (ISI) may involve non-identical processes.
Objective: This study aims to utilise combined TMS–EEG to more thoroughly characterise LICI at different ISIs, as the TMS-evoked EEG potential (TEP) can provide more direct insight into the cortical response to stimulation that is not subject to variations in spinal cord excitability that can confound the motor evoked potential (MEP).
Methods: In 12 subjects (22.6 ± 0.9 years), LICI was applied using two ISIs of 100 ms ($LICI_{100}$) and 150 ms ($LICI_{150}$), while TEPs were recorded using simultaneous high-definition EEG.
Results: Analysis of EEG data within a region of interest (C3 electrode) showed that test alone stimulation produced three consistent TEP peaks (corresponding to P30, N100 and P180) that were all significantly inhibited following paired-pulse stimulation. However, for P30, inhibition varied between LICI conditions, with reduced amplitude following $LICI_{100}$ ($P = 0.03$) but not $LICI_{150}$ ($P = 0.3$). In contrast, the N100 and P180 were significantly reduced by LICI at both intervals (all P-values < 0.05). In addition, topographical analyses suggested that the global change in P30, N40 and P180 differed between LICI conditions.
Conclusions: These findings suggest that $LICI_{100}$ and $LICI_{150}$ reflect complex measurements of cortical inhibition with differential contributions from comparable circuits.

Introduction

Within the central nervous system, inhibitory neurotransmission mediated by the activity of γ-aminobutyric acid (GABA) represents a fundamental component of normal function. Some important examples of this include the role of GABA in moderating synaptic plasticity [1], in mediating sensory acuity via surround inhibition [2–4] and in the generation of cortical oscillatory activity [5]. The functional importance of GABA is further illustrated by observations that GABAergic tone is modified in several different movement pathologies (see Ref. [6]) and psychiatric conditions [7,8]. In human subjects, paired-pulse transcranial magnetic stimulation (ppTMS) is a method which can provide an assessment of GABAergic function with a high temporal acuity. When applied over the primary motor cortex (M1), suprathreshold ppTMS at long (100–200 ms) interstimulus intervals (ISIs) produces a motor evoked potential (MEP) in peripheral muscles that is reduced in amplitude relative to the MEP produced by a single magnetic stimulus. This effect, referred to as long-interval intracortical inhibition (LICI [9]), is thought to be mediated by interactions between GABA type B ($GABA_B$) receptors activated by the first (conditioning) stimulus and corticospinal neurons activated by the second (test) stimulus [10–12].

Abbreviations: EEG, electroencephalography; EMG, electromyography; FDI, first dorsal interosseous; GABA, gamma-aminobutyric acid; ISI, interstimulus interval; LICI, long-interval intracortical inhibition; MEP, motor-evoked potential; MSO, maximum stimulator output; ppTMS, paired-pulse TMS; RMT, resting motor threshold; ROI, region of interest; SICI, short-interval intracortical inhibition; TBS, theta burst stimulation; TEP, TMS-evoked potential; TMS, transcranial magnetic stimulation.

* Corresponding author. Fax: + 61 8 8313 4398.
E-mail address: george.opie@adelaide.edu.au (G.M. Opie).

1935-861X/
http://dx.doi.org/10.1016/j.brs.2016.08.004

While LICI measurements have been obtained for more than 20 years, our understanding of the contributing cortical mechanisms is still relatively limited. This is exemplified by a gradually increasing body of evidence suggesting that the factors contributing to inhibition of the MEP may vary depending on the ISI. For example, previous studies have reported a divergent response of LICI at different ISIs to temporary ischaemia [13], cerebellar TBS [14] and ageing [15]. Furthermore, separate profiles of inhibitory recruitment have been reported at different intervals [16]; the inhibitory effect of LICI when applied 100 ms prior to SICI is reduced [17] or absent [18] when LICI precedes SICI by 150 ms, and LICI at 100 ms and 150 ms show differential task-related variations in inhibitory tone [17]. As changes in LICI have been associated with several different pathologies [6], and may be involved with aspects of motor control [17,19,20], it is important to gain a better understanding of the mechanisms reflected by this measurement at different ISIs.

One technique increasingly utilised to investigate the response to brain stimulation is TMS–electroencephalography coregistration (TMS–EEG). TMS–EEG facilitates a direct assessment of the cortical response to stimulation, removing the confounding influence of variations in spinal cord excitability that is known to affect conventional MEP measurements. In addition, combining these two methods provides significantly more information about the local and global responses to ppTMS than can be derived from the MEP [21,22]. For LICI, previous studies utilising TMS–EEG in M1 have identified cortical indices of inhibition within TMS-evoked EEG potentials (TEPs), with specific TEP peaks produced by the test stimulus being reduced in amplitude when a conditioning stimulus is applied 100 ms earlier [23]. Furthermore, by varying stimulus intensities [24] and applying pharmacological interventions [25], recent studies have also found that the modulation of individual TEP peaks following LICI applied with a 100 ms ISI likely reflects the inhibition of more than one mechanism. If the relative contribution of each of these mechanisms to the MEP inhibition observed following LICI were to vary as a function of ISI, changes in their individual influence may explain the divergent characteristics of LICI measurements at different ISIs. However, the cortical response to LICI at different intervals has not been investigated by previous research.

The main aim of the current study was therefore to investigate the local and global cortical mechanisms contributing to the inhibition observed when recording LICI at different ISIs. This was accomplished using combined TMS–EEG to record the response to LICI at 100 ms and 150 ms ISIs. Based on the TMS studies cited above, we expected that TMS–EEG indices of LICI would also differ between ISIs, which would suggest that LICI at these intervals reflect different mechanisms.

Materials and methods

12 young (mean ± SD: 22.6 ± 0.9) healthy subjects were recruited from the university and wider community to participate in the current study. Exclusion criteria included a history of neurological or psychiatric disease, or current use of psychoactive medication (sedatives, antipsychotics, antidepressants etc.). Assessments of hand preference using the Edinburgh Handedness Inventory [26] suggested that all subjects were, on average, right handed (laterality quotient: 0.75 ± 0.09). All experimentation was approved by the University of Adelaide Human Research Ethics Committee and conducted in accordance with the Declaration of Helsinki. Each subject provided written, informed consent prior to participation.

Experimental setup

For the duration of the experiment, subjects were seated in a comfortable chair with their hands resting on a cushion placed in their lap. Surface electromyography (EMG) was used to record responses from the first dorsal interosseous (FDI) muscle of the right hand. Two Ag–AgCl electrodes (1.5 cm diameter) were attached to the skin over the muscle in a belly-tendon montage, with a strap around the wrist grounding the electrodes. EMG was amplified (1000×) and band-pass filtered (20 Hz high pass, 1 kHz low pass) using a CED1902 (Cambridge Electronic Design, Cambridge, UK) before being digitised at 2 kHz using a CED1401 interface (Cambridge Electronic Design) and stored offline for analysis. EEG data were recorded using a cap with 59 sintered Ag–AgCl electrodes in standard 10–20 positions. The average of all recorded electrodes was used as reference for all channels. EEG data were acquired using an ASA-lab EEG system (ANT Neuro, Enschede, The Netherlands). Signals were amplified 20×, filtered (DC–0.27 × sampling rate) and digitised at 2048 Hz before being recorded on a computer for offline analysis. During each experiment, impedance was constantly checked and adjusted when necessary to be below 10 kΩ.

Transcranial magnetic stimulation

All stimulation was applied with the EEG cap in place. TMS was applied to the left primary motor cortex using a figure-of-eight coil (external wing diameter 9 cm) with two monophasic Magstim 200^2 magnetic stimulators connected via a Bistim unit (Magstim, Dyfed, UK). The coil was held tangentially to the scalp at an angle of 45° to the sagittal plane, with the handle pointed backwards and laterally, producing an anteriorly directed current flow in the brain. The coil was positioned on the scalp over the location producing an optimum response in the relaxed FDI muscle. This location was marked on the cap for reference and continually checked throughout the experiment. During all stimulation, TMS was delivered at a rate of 0.2 Hz with a 10% variance between trials.

Resting motor threshold (RMT) was obtained in FDI while the TMS coil was placed at the optimum location over primary motor cortex. RMT was defined as the lowest stimulus intensity producing a response amplitude ≥50 μV in at least three out of five trials in resting FDI muscle, and expressed relative to the maximum stimulator output (MSO). Long-interval intracortical inhibition (LICI) was assessed using conditioning and test stimuli both set to 120% RMT, and two interstimulus intervals (ISIs) of 100 ($LICI_{100}$) and 150 ($LICI_{150}$) ms. During the assessment of LICI, subjects received a total of 84 single (test alone) and 168 paired (84 $LICI_{100}$, 84 $LICI_{150}$) TMS stimuli. To avoid a loss of subject attention, these stimuli were applied over 7 blocks of 36 stimuli, with each block including equal numbers of each stimulus condition applied in a pseudo-randomised order. To minimise the auditory-evoked potentials resulting from the TMS discharge, subjects listened to white noise played through ear plugs (<70 dB in each ear) for the duration of each stimulus block.

Data analysis

Analysis of EMG data was completed manually via visual inspection of offline recordings. All traces showing voluntary EMG activity prior to stimulation were removed from analysis. MEP amplitudes for each trial were measured peak-to-peak and expressed in mV. Paired-pulse measurements of LICI were quantified by expressing the difference between the average conditioned and unconditioned MEP amplitude as a percentage of the average unconditioned MEP amplitude within each recording block. A grand average LICI measurement was then calculated for each subject by averaging the LICI measurements from each recording block.

EEG data were analysed according to previously reported procedures [27] using EEGLAB [28], fieldtrip [29] and custom written scripts on the MATLAB platform (R2013a, The Mathworks, USA). Data from all blocks were merged into a single file, epoched around the

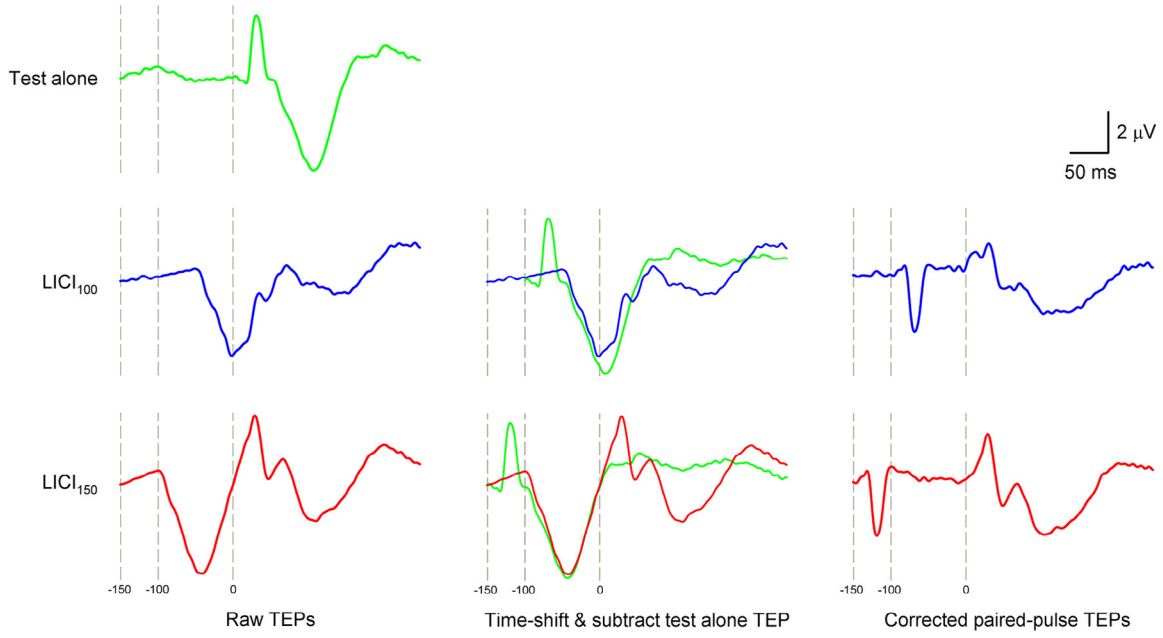

Figure 1. Paired-pulse TEP correction procedure. The TEP generated by the conditioning stimulus can be clearly visualised in the $LICI_{100}$ (*blue line*) and $LICI_{150}$ (*red line*) raw data traces (*left column*), and is most apparent as a large negative deflection at the time of test stimulation (i.e., 0 ms) for $LICI_{100}$, and 50 ms prior to the test stimulus for $LICI_{150}$. The confounding influence of this potential was removed from paired-pulse data by time shifting the raw TEP generated by test alone stimulation (*green line*) to coincide with the conditioning stimulus for each LICI condition (–100 for $LICI_{100}$, –150 for $LICI_{150}$) and then subtracting it from the raw TEPs generated by $LICI_{100}$ and $LICI_{150}$ (*middle column*), resulting in corrected paired-pulse TEPs (*right column*). (For interpretation of the references to colour in this figure legend, the reader is referred to the web version of this article.)

TMS pulse (±1000 ms), baseline corrected (–650 to –200 ms) and bad channels were removed. Large amplitude artefacts associated with the TMS pulse were then removed from each epoch. Depending on the stimulus condition, data were cut from –1.5 to 20 ms (test pulse; all conditions), from –110 to –50 ms ($LICI_{100}$ conditioning stimulus) or from –160 to –100 ms ($LICI_{150}$ conditioning stimulus), with the missing sections of data replaced using cubic interpolation. Following this, an initial independent component analysis (ICA) was run using the FastICA algorithm [30], and a single large component representing the tail end of the TMS-associated muscle artefact was identified and removed [27]. Data were then band-pass (1–100 Hz) and notch (50 Hz) filtered using the 'eegfiltnew' function within EEGLAB, before being visually inspected for trials containing anomalous activity (e.g., EMG bursts from facial muscle activation or noise from electrode movement). A second FastICA analysis was then run, with components relating to stimulus decay, blinks/eye-movements, auditory-evoked potentials and other noise being identified and removed. Epochs were then split into stimulus conditions for quantification of TMS evoked potentials (TEPs). For all analyses, the TEP generated by test alone stimulation was compared to that generated following $LICI_{100}$ and $LICI_{150}$. However, prior to quantification of paired-pulse TEPs, a correction procedure was carried out to remove the TEP generated by the conditioning stimulus from the TEP generated by the test stimulus [23,25,31]. This was achieved by time-shifting the TEP generated by test alone stimulation to coincide with the application of each conditioning stimulus, and subtracting it from the paired-pulse data (Fig. 1; this was performed separately for $LICI_{100}$ and $LICI_{150}$ data). As all of the test alone TEP trace from 0 to 1000 ms was time shifted, only the last 100–150 ms (depending on the LICI condition) of the paired-pulse TEP was not corrected. However, data at this latency were not included in any of the analyses and therefore could not have influenced our findings.

TEPs were quantified according to both a region of interest (ROI) analysis and global scalp analysis. During ROI analysis, the TEP components P30, N40, P60, N100 and P180 were investigated at the C3 electrode (closest channel to the site of stimulation). For the test alone condition, these components were quantified by assessing the maximum positive peaks between 25–40 ms (P30), 45–75 ms (P60) and 160–220 ms (P180), and maximum negative peaks between 25–55 ms (N40) and 85–145 ms (N100). The amplitude of each peak during both LICI conditions was then assessed at the peak latency identified within the test alone condition. For each peak component in all conditions, the maximum amplitude was calculated as the average of the signal ±5 ms from the maximum peak. The effects of LICI on each component were calculated by normalising the difference between the peaks resulting from test alone and paired-pulse stimulation to the overall size of the TEP (from 25 to 220 ms) generated by test alone stimulation. For normalisation of positive peaks, test TEP size was calculated as $TEP_{max} - TEP_{min}$, whereas this was reversed to $TEP_{min} - TEP_{max}$ for normalisation of negative peaks. Subsequently, larger values reflect greater inhibition for all normalised indices of LICI, including those measured using the MEP. To identify peaks that were absent within the ROI but present globally, the global mean field amplitude (GMFA) was calculated [32]. This analysis utilised the same time windows and quantification methods as those that were applied for ROI analysis.

The N100 produced by the conditioning stimulus has been previously implicated as a factor contributing to the inhibitory effects observed during both conventional and TMS–EEG measures of LICI [24]. To further investigate the possibility that different mechanisms might contribute to LICI at different ISIs, we therefore quantified the N100 produced by $LICI_{100}$ and $LICI_{150}$ conditioning stimuli. This was accomplished by calculating the average first derivative over the 10 ms prior to the N100 waveform produced by the conditioning stimulus in each LICI state (i.e., ~0–10 ms prior to the test stimulus for $LICI_{100}$ and 50–60 ms prior to the test stimulus for $LICI_{150}$). This was calculated using uncorrected paired-pulse TEP data.

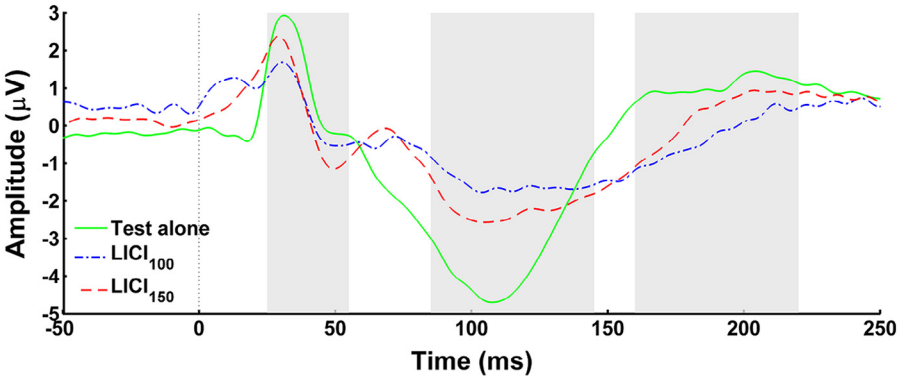

Figure 2. TEP peaks recorded following test alone and paired-pulse stimulation. Data show the response to test alone stimulation (green line), $LICI_{100}$ (blue line) and $LICI_{150}$ (red line) recorded at the C3 electrode and averaged over all subjects. Shaded boxes demonstrate the time periods used to identify each peak. (For interpretation of the references to colour in this figure legend, the reader is referred to the web version of this article.)

Statistical analysis

Normality of distribution was assessed using Kolmogorov–Smirnov tests, the results of which suggested that MEP and non-normalised ROI data failed to meet assumptions of normality, whereas normalised ROI data were normally distributed. The amplitude of the MEP and each TEP component was compared between stimulus conditions (test alone, $LICI_{100}$, $LICI_{150}$) using individual Friedman tests. Following a significant main effect, pair-wise comparisons were made using Dunn–Bonferroni tests [33]. Normalised MEP measures of LICI were compared between ISIs using a Mann–Whitney U test, whereas normalised LICI values for each TEP component were compared between ISIs using individual paired t-tests. Interactions between data recorded in each stimulus condition were further investigated using Spearman's rank correlations. Global TEP characteristics (i.e., the TEP response at each electrode) were compared between stimulus conditions using non-parametric cluster based permutation statistics, which provides a robust protection against multiple comparison errors [34]. Clusters were defined as two or more neighbouring electrodes that demonstrated a t-statistic with an associated P-value < 0.05. Identified clusters were then subjected to cluster-based analysis using a permutation distribution generated with a Monte Carlo method (2000 permutations). A cluster was deemed significant if the cluster-statistic (i.e., the largest t-statistic in each cluster) exceeded $P < 0.05$ when compared to the permutation distribution. Cluster statistics were used to compare TEP amplitude following $LICI_{100}$ and $LICI_{150}$ to the amplitude of the TEP elicited by the test alone stimulus. They were also used to compare normalised LICI measurements between $LICI_{100}$ and $LICI_{150}$. For both analyses, comparisons utilised all electrodes and were carried out separately for each TEP peak using data averaged over the mean peak time (derived from test alone stimulation recorded at C3) ±5 ms. Unless otherwise stated, data are presented as mean ± standard error of the mean (SEM).

Results

All subjects completed the experiment in full and without adverse reaction. The average RMT was 55.8 ± 2.2% MSO, while the average test MEP amplitude was 1.38 mV. Analysis of MEP data showed that the response to LICI varied between stimulus conditions ($P < 0.001$), with post hoc testing showing that test MEP amplitude was reduced following $LICI_{100}$ (0.10 mV, $P < 0.001$) and $LICI_{150}$ (0.46 mV, $P = 0.007$), but that there was no difference between ISIs ($P = 0.6$). Furthermore, normalised LICI values were also not different between intervals ($LICI_{100}$, 88.8 ± 4.1%; $LICI_{150}$, 74.5 ± 8.0%; $P = 0.08$).

ROI analysis

Test alone stimulation produced 5 identifiable peaks in the EEG data; 3 positive deflections at 31.2 ± 1.4 ms (P30), 58.4 ± 1.2 ms (P60) and 195.3 ± 5.8 ms (P180), and 2 negative deflections at 43.5 ± 2.2 ms (N40) and 105.0 ± 3.0 ms (N100). Of these, P30, N100 and P180 were observed in all subjects, whereas N40 was seen in 9/12 subjects and P60 in 8/12 subjects. Subsequent analysis therefore focussed on the more reliable P30, N100 and P180 potentials (Fig. 2). The amplitude of each peak following test alone and paired-pulse stimulation is shown in Fig. 3. For P30, a significant effect of stimulus condition was found ($P = 0.03$; Fig. 3A), with post hoc analysis showing a reduced amplitude relative to the response to test alone stimulation following $LICI_{100}$ ($P = 0.03$) but not $LICI_{150}$ ($P = 0.9$). Furthermore, there was no difference in amplitude between LICI conditions ($P = 0.3$). While the N100 was also affected by stimulus condition ($P < 0.001$; Fig. 3C), post hoc testing showed that the amplitude of this potential was reduced relative to the test alone response following both $LICI_{100}$ ($P < 0.001$) and $LICI_{150}$ ($P = 0.01$), but was not different between LICI conditions ($P = 0.9$). This was also the case for the P180, with a significant effect of stimulus condition ($P = 0.001$; Fig. 3E) driven by the response following both paired-pulse conditions being reduced relative to the response following test alone stimulation ($LICI_{100}$, $P = 0.001$; $LICI_{150}$, $P = 0.04$), but no difference between LICI conditions ($P = 0.7$). To further compare the magnitude of inhibition between each interval, a normalised index of LICI was calculated (see the Materials and methods section). This index showed that, compared to $LICI_{150}$, $LICI_{100}$ produced increased inhibition of P30 ($P = 0.04$, Fig. 3B), and a tendency towards increased inhibition of N100 ($P = 0.06$, Fig. 3D), but that there was no difference in the inhibition of P180 ($P = 0.1$, Fig. 3F).

Correlations between the slope of the N100 produced by the conditioning stimulus in each LICI condition, and the associated TEP/MEP inhibition for that condition are shown in Table 1. The significant

Table 1
Correlations between TEP/MEP LICI measurements and the slope of the N100 produced by $LICI_{100}$ and $LICI_{150}$ conditioning stimuli.

	$LICI_{100}$ N100 slope			$LICI_{150}$ N100 slope	
	Coefficient (ρ)	*P*-value		Coefficient (ρ)	*P*-value
$LICI_{100}$			$LICI_{150}$		
P30	–0.3	0.3	P30	–0.4	0.2
N100	–0.01	0.9	N100	0.2	0.5
P180	0.6	0.04	P180	–0.05	0.9
MEP	–0.7	0.03	MEP	0.06	0.9

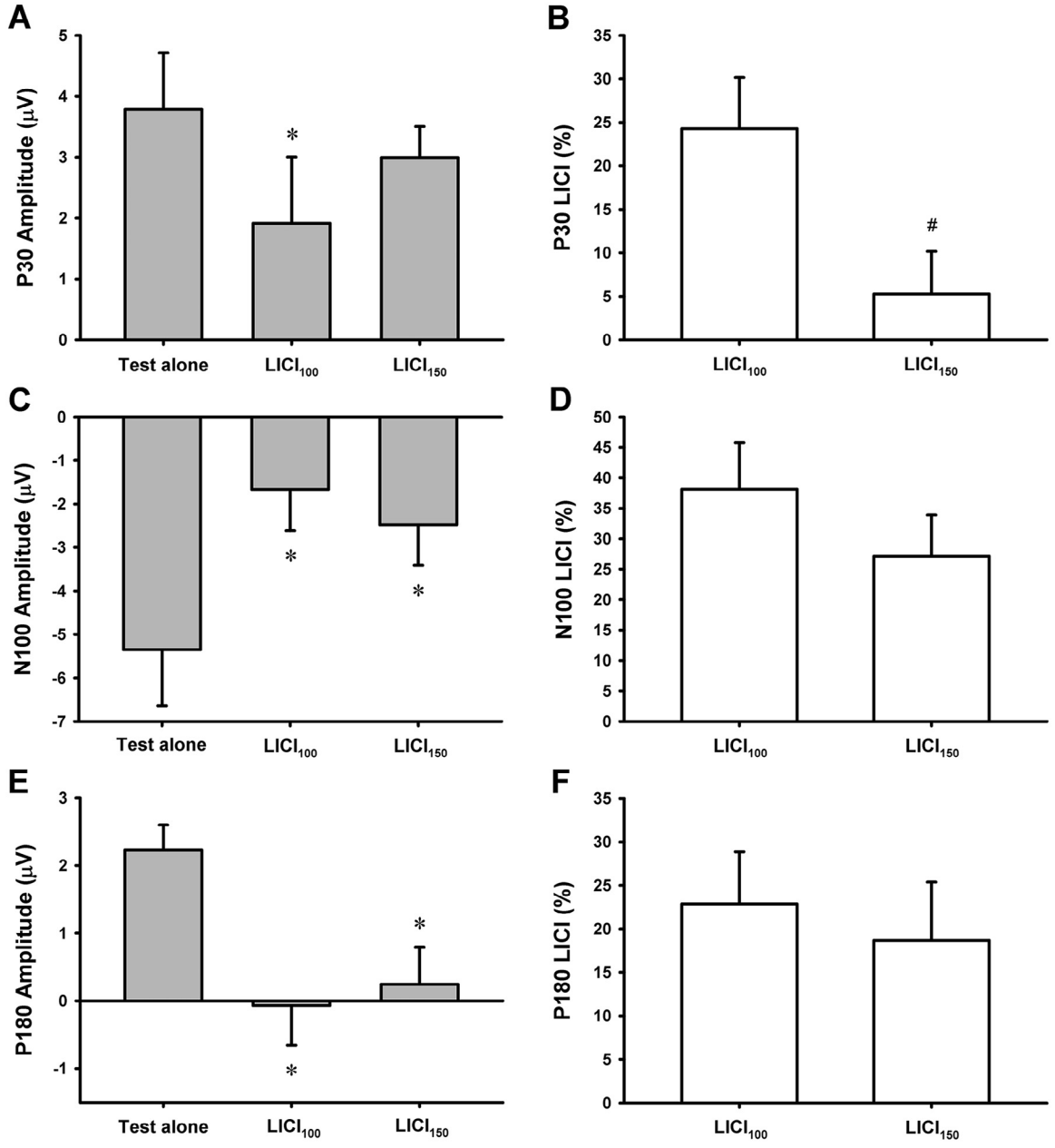

Figure 3. Amplitude of TEP peaks following test alone and paired-pulse TMS. Data show the absolute (*left column*) and normalised (*right column*) TEP data for P30 (A, B), N100 (C, D) and P180 (E, F) peaks following test alone and paired-pulse TMS. For normalised data, 0% represents no inhibition of the test TEP. $^{*}P < 0.05$ when compared to the amplitude produced by test alone stimulation. $^{\#}P < 0.05$ when compared to $LICI_{100}$.

positive association between the $LICI_{100}$ N100 slope and $LICI_{100}$ of P180 suggests that a more positive N100 slope is associated with greater inhibition of P180 at the 100 ms interval. However, significant negative associations between the $LICI_{100}$ N100 slope and MEP measures of $LICI_{100}$ suggest that a more negative $LICI_{100}$ N100 slope is associated with stronger inhibition of the MEP at the 100 ms interval. Correlations between the TEP/MEP inhibition produced by each LICI interval are shown in Table 2. These were performed to identify if common mechanisms contributed to the inhibition of each TEP peak, with significant relationships between conditions interpreted as reflective of similar processes. The significant positive associations between intervals for LICI of N100, P180 and the MEP suggest that an increase in inhibition at one interval is associated with an increase in inhibition at the other interval.

Cluster-based analysis

The effects of LICI on global TEP characteristics was investigated using cluster-based analysis [25,31]. In contrast to ROI analysis,

Table 2
Correlations between TEP/MEP inhibition produced by $LICI_{100}$ and $LICI_{150}$.

	Coefficient (ρ)	*P*-value
P30	–0.3	0.3
N100	0.8	0.01
P180	0.9	0.005
MEP	0.9	0.004

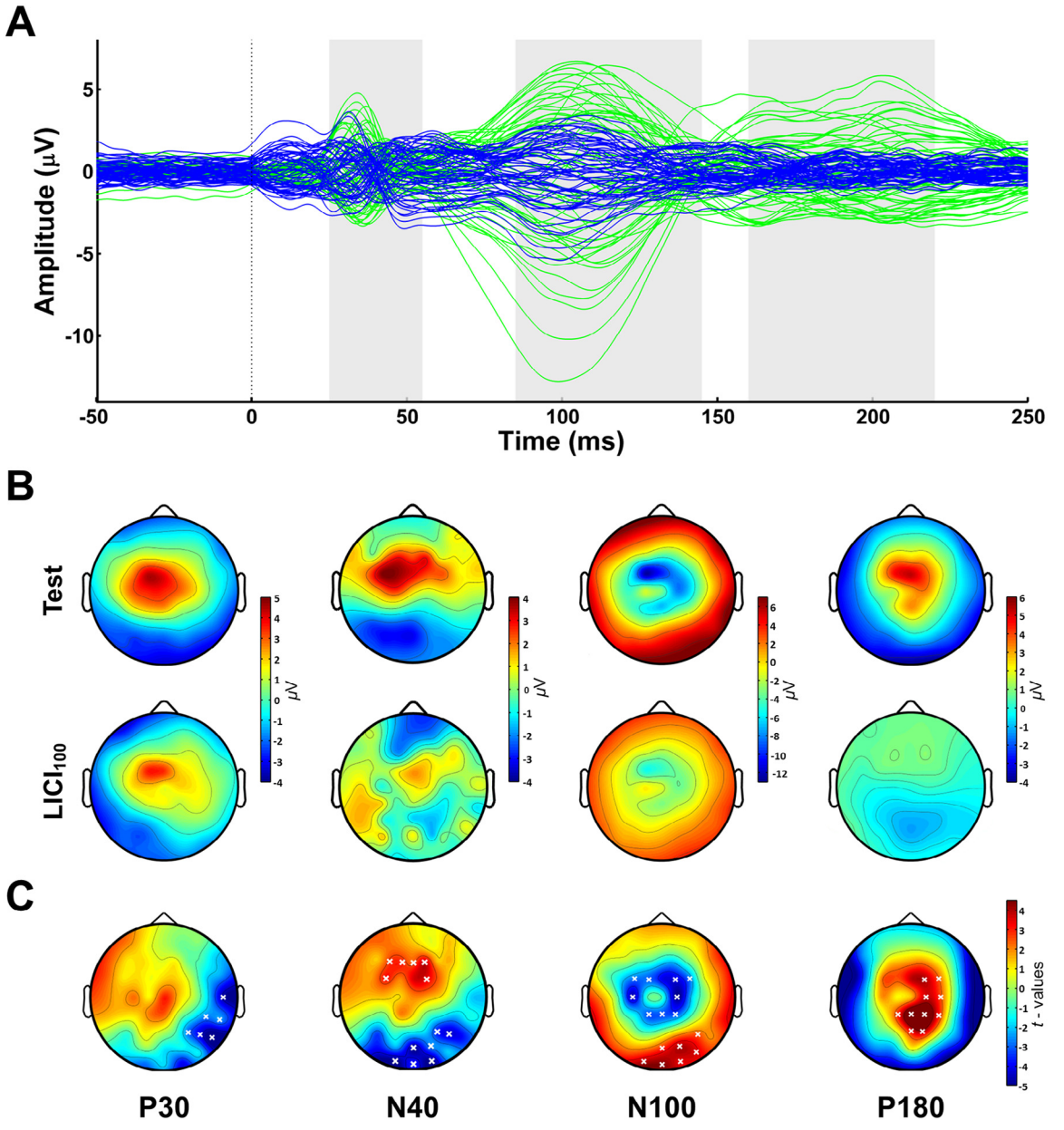

Figure 4. Spatiotemporal TEP evolution following test alone and $LICI_{100}$ stimulation. (A) Butterfly plots showing the response to test alone stimulation (green lines) and $LICI_{100}$ (blue lines) averaged across all subjects at each electrode. Shaded boxes demonstrate the time periods used to identify each peak; as the P30 and N40 potentials were investigated within overlapping time windows, these are both represented by the left box. The dotted vertical line represents the time at which the test pulse was applied. (B) Topoplots showing scalp potentials associated with each peak of interest (i.e., P30, N40, N100 and P180) following test alone and $LICI_{100}$ stimulation. (C) Topoplots showing t-statistics derived from cluster-based comparisons between the test alone and $LICI_{100}$ conditions. White crosses identify electrodes contributing to significant clusters. (For interpretation of the references to colour in this figure legend, the reader is referred to the web version of this article.)

the N40 was reliably present in GMFA analysis (observed in all subjects). This potential was therefore included within global scalp analysis. Comparisons were made between the responses recorded following test alone and paired-pulse stimulation (i.e., test alone compared with $LICI_{100}$ and test alone compared with $LICI_{150}$), in addition to between normalised LICI values for each ISI (i.e., $LICI_{100}$ compared with $LICI_{150}$). Comparisons between the test alone and $LICI_{100}$ topographies showed significant clusters over contralateral temporal-parietal electrodes associated with the P30 latency ($P = 0.02$), over frontal-central ($P = 0.03$) and occipital/contralateral parietal ($P = 0.005$) electrodes associated with the N40 latency, over central ($P = 0.002$) and occipital/contralateral parietal ($P = 0.008$) electrodes associated with the N100 latency and over central ($P = 0.003$) electrodes associated with the P180 latency (Fig. 4C). Comparisons between the test alone and $LICI_{150}$ topographies showed that a single cluster associated with the P30 latency failed to reach significance when compared to the Monte Carlo distribution ($P = 0.07$). However, significant clusters were found over frontal central ($P = 0.02$) and occipital/contralateral temporal-parietal ($P = 0.003$) electrodes associated with the N40 latency, over central ($P = 0.0005$) and occipital ($P = 0.008$) electrodes associated with N100 latency, and over posterior central ($P = 0.006$) and ipsilateral frontal-parietal ($P = 0.02$) electrodes associated with the P180 latency (Fig. 5C). Comparisons between the global topographies of each LICI condition failed to identify significant clusters associated with any of the peaks of interest (Fig. 6).

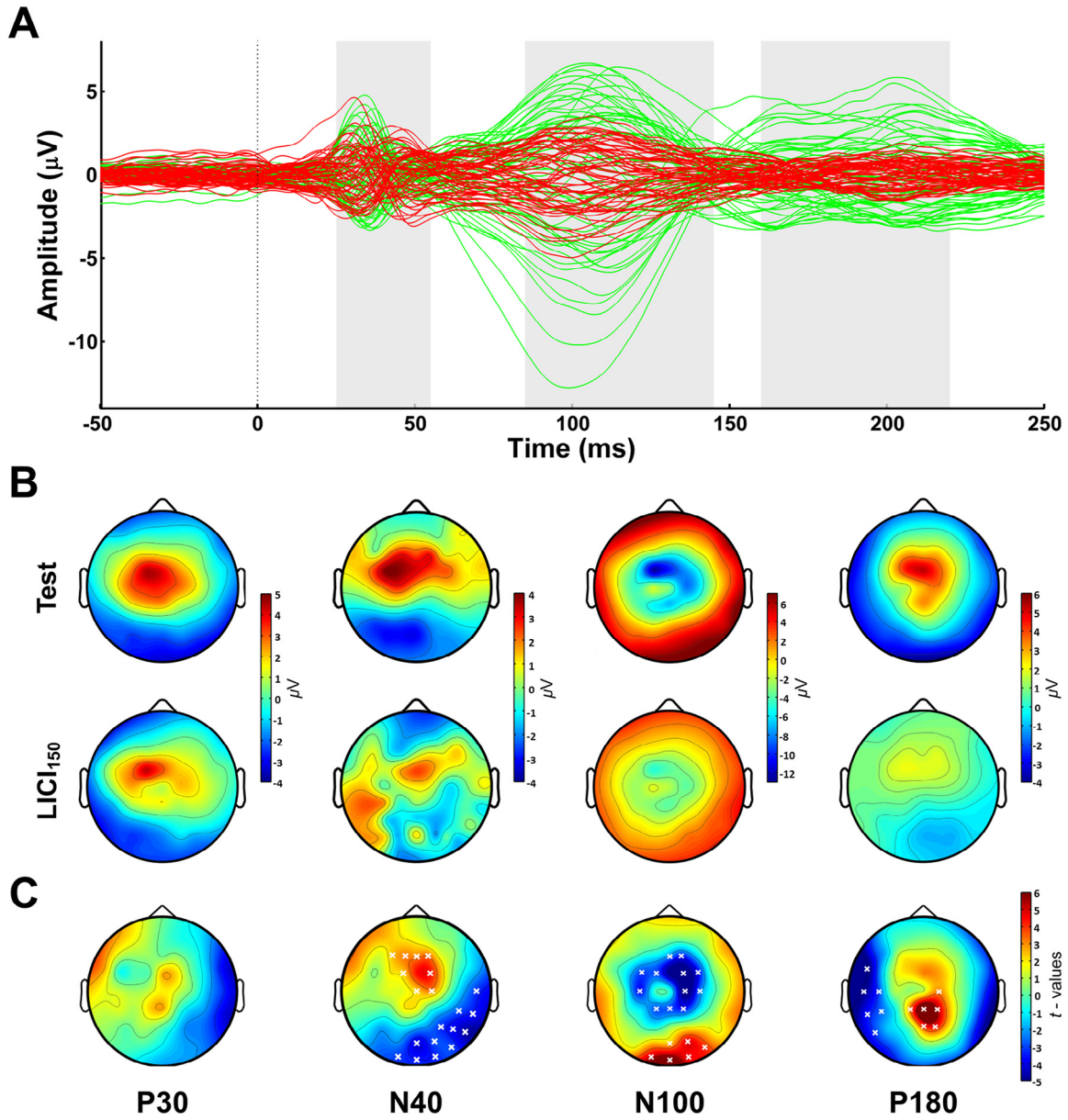

Figure 5. Spatiotemporal TEP evolution following Test alone and $LICI_{150}$ stimulation. (A) Butterfly plots showing the response to test alone stimulation (green lines) and $LICI_{150}$ (red lines) averaged across all subjects at each electrode. Shaded boxes demonstrate the time periods used to identify each peak; as the P30 and N40 potentials were investigated within overlapping time windows, these are both represented by the left box. The dotted vertical line represents the time at which the test pulse was applied. (B) Topoplots showing scalp potentials associated with each peak of interest (i.e., P30, N40, N100 and P180) following test alone and $LICI_{150}$ stimulation. (C) Topoplots showing t-statistics derived from cluster-based comparisons between the test alone and $LICI_{150}$ conditions. White crosses identify electrodes contributing to significant clusters. (For interpretation of the references to colour in this figure legend, the reader is referred to the web version of this article.)

Discussion

For most studies using LICI to investigate $GABA_B$ mediated inhibition, an ISI of 100 ms is generally used, as this is thought to produce maximum inhibition of the MEP [9]. However, LICI can be assessed over a broad range of intervals [9,35], with measurements at different ISIs often assumed to reflect comparable mechanisms. Within the current study, we found several lines of evidence suggesting similarities between the mechanisms contributing to LICI at each ISI, including correlations between the slope of the N100 produced by the $LICI_{100}$ conditioning stimulus and MEP inhibition produced in both LICI conditions (Table 1); correlations between LICI conditions for inhibition of the late TEP peaks (N100 and P180, Table 2), and no topographical difference between conditions for normalised LICI values (Fig. 6). However, we also found several lines of evidence suggesting that the extent to which these comparable mechanisms are activated differs between LICI conditions, including differential local inhibition of P30 by each LICI condition (Fig. 3A, B); differential global inhibition of P30 and P180 by each LICI condition (Figs. 4C and 5C); a lack of correlation between LICI conditions for the magnitude of P30 inhibition (Table 2) and significant correlations between MEP inhibition and the slope of the N100 produced by the conditioning stimulus for $LICI_{100}$ but not $LICI_{150}$ (Table 1). Taken together, these findings suggest that $LICI_{100}$ and $LICI_{150}$ likely represent complex measurements involving composite and differential activation of common mechanisms.

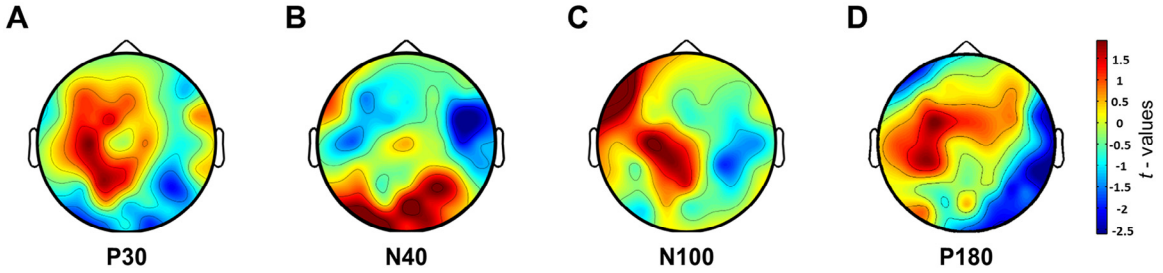

Figure 6. Topographic differences between LICI measured at each ISI. Topoplots show the t-statistics derived from cluster-based comparisons between $LICI_{100}$ and $LICI_{150}$ at time points associated with P30 (A), N40 (B), N100 (C) and P180 (D). No significant clusters were identified at any time point.

Mechanisms of LICI

The mechanisms contributing to inhibition of the MEP following application of LICI have been extensively investigated. While LICI at ISIs < 50 ms is generally thought to reflect the influence of spinal mechanisms, inhibitory effects at longer ISIs (i.e., >100 ms) are more likely cortical in nature [36,37]. This is supported by studies showing reductions in the amplitude of the late indirect (I) waves following LICI [36,37]. Furthermore, several studies using pharmacological interventions to modulate GABAergic tone suggest that LICI is mediated by activation of the metabotropic $GABA_B$ receptor [10,11,38].

While conventional TMS–EMG measures have provided some physiological insight into the mechanisms of LICI, TMS–EEG is emerging as a powerful technique with which it is possible to probe further the physiological basis of LICI effects. Using TMS–EEG, several studies have shown that LICI is associated with reduced excitability in both motor and non-motor areas of cortex [23,39–41]. For the primary motor cortex, the magnitude of this inhibition correlates with inhibition of the MEP, demonstrating the involvement of mechanisms comparable to those reflected by conventional LICI measurements. Furthermore, a recent study using pharmacological interventions has observed a potentiation of the cortical effects of LICI following baclofen intake [25], providing strong support for a mediatory role of the $GABA_B$ receptor in the effects of LICI.

Within the current study, TEPs recorded at the C3 electrode were reduced in amplitude following application of LICI. This was observed for the P30 (for $LICI_{100}$ only), N100 and P180, all of which have been previously reported to be reduced by LICI [24,25]. Furthermore, correlational analyses found significant relationships between the slope of the N100 produced by the conditioning stimulus and inhibition of the MEP. Interestingly, this relationship was observed for $LICI_{100}$ but not $LICI_{150}$, suggesting a reduced role of the N100 in mediating the MEP inhibition observed following $LICI_{150}$. Despite this, our findings support previous suggestions that TMS–EEG indices of LICI reflect engagement of similar mechanisms to those responsible for MEP suppression, providing further evidence for the reliability of TMS–EEG as a measure of cortical inhibition.

Cortical effects of $LICI_{100}$ and $LICI_{150}$

While the mechanisms underlying the generation of each TEP peak are not completely understood, contributions from independent cortical mechanisms are likely [24,25,42]. For P30, several lines of evidence implicate a role of cortical excitatory processes associated with the TMS pulse, including observations that P30 amplitude correlates with MEP amplitude [43], that P30 and the MEP both demonstrate sigmoidal recruitment curves [32,44], that GABAergic potentiation does not modulate P30 amplitude [42] and that LICI of P30 correlates with LICI of the MEP [24]. Subsequently, LICI of P30 has been interpreted as a reflection of the cortical inhibitory processes underlying the reductions in MEP amplitude associated with LICI [24], which are thought to include activation of post-synaptic $GABA_B$ receptors [11,38]. However, as potentiation of $GABA_B$-mediated activity failed to modulate LICI of P30 [25], this may not be the case. Despite this, as our results demonstrate that P30 was inhibited by $LICI_{100}$ but not $LICI_{150}$, whereas MEP inhibition was not different between intervals, the factors contributing to inhibition of the MEP must be multifactorial.

In addition to local differences between intervals for inhibition of P30, topographical analyses also suggested that application of $LICI_{100}$ but not $LICI_{150}$ was associated with a reduced negative potential within contralateral cortical areas (Figs. 4C and 5C). While the reason for this is not currently clear, interhemispheric inhibitory connections which have been well documented by previous TMS studies [45–47] may be important. These connections are thought to consist of excitatory transcallosal projections that synapse with local inhibitory neurons within the contralateral hemisphere [48], the activation of which results in inhibition in contralateral cortex. The reduced amplitude of negative TMS–EEG potentials observed within contralateral cortex following $LICI_{100}$ may therefore represent an inhibition of the transcallosal excitatory neurons associated with this pathway. This suggestion is supported by previous observations that the circuits mediating LICI and interhemispheric inhibition have a negative interaction [48]. The reason that $LICI_{150}$ failed to produce similar effects is also unclear. However, as $LICI_{150}$ produced a similarly located cluster that just failed to reach significance ($P = 0.07$), and the topoplots of P30 were comparable between intervals (Figs. 4B and 5B), it seems possible that the lack of change within contralateral areas following $LICI_{150}$ may reflect a resolution of the inhibitory effects of the conditioning stimulus within the site of stimulation.

As N40 could not be reliably identified in all subjects at the C3 electrode, ROI analysis of this potential was not performed. However, GMFA data suggested it was reliably present outside of the ROI, and it was therefore included within the global scalp analysis. In support of previous findings [25], the N40 was significantly reduced by LICI (Figs. 4C and 5C). Interestingly, comparisons between the test alone and LICI topographies showed that inhibition of N40 over contralateral temporal/parietal areas reached significance following $LICI_{150}$ but not $LICI_{100}$. The significance of this greater inhibition of N40 following $LICI_{150}$ is currently unclear.

While the mechanisms contributing to the P30 and N40 are poorly understood, strong evidence suggests that the N100 reflects activation of cortical inhibitory processes (for review, see Ref. [21]), most likely involving activation of the $GABA_B$ receptor [42]. As a reduction in N100 amplitude should therefore represent reduced inhibitory tone, the decreased N100 observed following LICI is counterintuitive. However, it has been suggested that LICI of N100 may reflect the activation of pre-synaptic $GABA_B$ receptors [24], which decrease GABA release from the pre-synaptic terminal [49], resulting in reduced inhibition. In the current study, there was a tendency for inhibition

of the N100 to be larger following $LICI_{100}$ than $LICI_{150}$, although this failed to reach a conventional level of significance ($P = 0.06$). This suggests that $LICI_{100}$ is associated with increased activation of both pre-synaptic and post-synaptic (see discussion of P30 above) $GABA_B$ receptors. Interestingly, as post-synaptic inhibition had resolved 150 ms after the conditioning stimulus (i.e., P30 was not inhibited by $LICI_{150}$), whereas presynaptic inhibition was still present (i.e., N100 was inhibited by $LICI_{150}$), our findings are consistent with suggestions that pre-synaptic inhibition has a broader time-scale than post-synaptic inhibition [35]. Furthermore, they also support observations from our group that the interaction between SICI and LICI, which is thought to reflect activation of pre-synaptic $GABA_B$ receptors, tends to be reduced at 150 ms [17].

The mechanisms contributing to the generation of P180 have received considerably less attention than other potentials. This long-latency response can have a contribution from the auditory evoked activity associated with the click produced by the TMS pulse [50,51]. However, this confounding influence is significantly reduced by white noise masking during stimulation [52], in addition to the use of independent component analysis [27], both of which were utilised within the current study. Furthermore, as the P180 can still be elicited in deaf subjects [52], and is significantly reduced in individuals with progressive myoclonus epilepsy [53], it seems likely that it has contributions from TMS-induced cortical activity. Observations from the current and previous [25] studies that P180 is strongly reduced by application of LICI provide further support for this suggestion. While the inhibition of P180 was not different between intervals at the C3 electrode, global scalp analysis identified differences between test alone and $LICI_{150}$ (but not $LICI_{100}$) topographies over ipsilateral frontal-parietal electrodes, suggesting increased global inhibitory effects of $LICI_{150}$ on P180.

In conclusion, our findings suggest that the cortical indices of $LICI_{100}$ and $LICI_{150}$ are characterised by differential local and global changes in early and late TEP components. These findings suggest that the LICI paradigm is associated with complex patterns of cortical activity that likely reflect composite activation of multiple cortical processes. Furthermore, while our findings do not suggest that the mechanisms involved differ between intervals, they do suggest that the relative contributions of these comparable mechanisms to the associated reductions in MEP amplitude are likely varied over time. In particular, $LICI_{100}$ may be associated with activation of both pre- and post-synaptic $GABA_B$ receptors, whereas $LICI_{150}$ seems to be more purely reflective of pre-synaptic $GABA_B$ receptor activation. This suggests that caution is required when interpreting and comparing conventional MEP measures of LICI at different intervals.

References

[1] Paulsen O, Moser E. A model of hippocampal memory encoding and retrieval: GABAergic control of synaptic plasticity. Trends Neurosci 1998;21:273–8.
[2] Vučinić D, Cohen LB, Kosmidis EK. Interglomerular center-surround inhibition shapes odorant-evoked input to the mouse olfactory bulb in vivo. J Neurophysiol 2006;95:1881–7.
[3] Kyriazi H, Carvell G, Brumburg J, Simons D. Quantitative effects of GABA and bicuculline meth on receptive field properties of neurons in real and simulated whisker barrels. J Neurophysiol 1996;75:547–60.
[4] Binns K, Salt T. Different roles for GABAA and GABAB receptors in visual processing in the rat superior colliculus. J Physiol (Lond) 1997;504:629–39.
[5] Mann EO, Paulsen O. Role of GABAergic inhibition in hippocampal network oscillations. Trends Neurosci 2007;30:343–9.
[6] Berardelli A, Abbruzzese G, Chen R, Orth M, Ridding MC, Stinear C, et al. Consensus paper on short-interval intracortical inhibition and other transcranial magnetic stimulation intracortical paradigms in movement disorders. Brain Stimul 2008;1:183–91.
[7] Benes FM, Berretta S. GABAergic interneurons: implications for understanding schizophrenia and bipolar disorder. Neuropsychopharmacology 2001;25:1–27.
[8] Lewis DA, Hashimoto T, Volk DW. Cortical inhibitory neurons and schizophrenia. Nat Rev Neurosci 2005;6:312–24.
[9] Valls-Sole J, Pascual-Leone A, Wassermann EM, Hallett M. Human motor evoked responses to paired transcranial magnetic stimuli. Electroencephalogr Clin Neurophysiol 1992;85:355–64.
[10] Werhahn KJ, Kunesch E, Noachtar S, Benecke R, Classen J. Differential effects on motorcortical inhibition induced by blockade of GABA uptake in humans. J Physiol (Lond) 1999;517:591–7.
[11] McDonnell MN, Orekhov Y, Ziemann U. The role of GABA(B) receptors in intracortical inhibition in the human motor cortex. Exp Brain Res 2006;173:86–93.
[12] Rossini P, Burke D, Chen R, Cohen L, Daskalakis Z, Di Iorio R, et al. Non-invasive electrical and magnetic stimulation of the brain, spinal cord, roots and peripheral nerves: basic principles and procedures for routine clinical and research application. An updated report from an IFCN Committee. Clin Neurophysiol 2015;126:1071–107.
[13] Vallence A-M, Reilly K, Hammond G. Excitability of intracortical inhibitory and facilitatory circuits during ischemic nerve block. Restor Neurol Neurosci 2012;30:345–54.
[14] Koch G, Mori F, Marconi B, Codecà C, Pecchioli C, Salerno S, et al. Changes in intracortical circuits of the human motor cortex following theta burst stimulation of the lateral cerebellum. Clin Neurophysiol 2008;119:2559–69.
[15] Opie GM, Ridding MC, Semmler JG. Age-related differences in pre- and post-synaptic motor cortex inhibition are task dependent. Brain Stimul 2015;8:926–36.
[16] Vallence A-M, Schneider LA, Pitcher JB, Ridding MC. Long-interval facilitation and inhibition are differentially affected by conditioning stimulus intensity over different time courses. Neurosci Lett 2014;570:114–18.
[17] Opie GM, Ridding MC, Semmler JG. Task-related changes in intracortical inhibition assessed with paired-and triple-pulse transcranial magnetic stimulation. J Neurophysiol 2015;113:1470–9.
[18] Chu J, Gunraj C, Chen R. Possible differences between the time courses of presynaptic and postsynaptic GABAB mediated inhibition in the human motor cortex. Exp Brain Res 2008;184:571–7.
[19] Hammond G, Vallence AM. Modulation of long-interval intracortical inhibition and the silent period by voluntary contraction. Brain Res 2007;1158:63–70.
[20] Kouchtir-Devanne N, Capaday C, Cassim F, Derambure P, Devanne H. Task-dependent changes of motor cortical network excitability during precision grip compared to isolated finger contraction. J Neurophysiol 2012;107:1522–9.
[21] Rogasch NC, Fitzgerald PB. Assessing cortical network properties using TMS–EEG. Hum Brain Mapp 2013;34:1652–69.
[22] Ilmoniemi RJ, Kičić D. Methodology for combined TMS and EEG. Brain Topogr 2010;22:233–48.
[23] Daskalakis ZJ, Farzan F, Barr MS, Maller JJ, Chen R, Fitzgerald PB. Long-interval cortical inhibition from the dorsolateral prefrontal cortex: a TMS–EEG study. Neuropsychopharmacology 2008;33:2860–9.
[24] Rogasch NC, Daskalakis ZJ, Fitzgerald PB. Mechanisms underlying long-interval cortical inhibition in the human motor cortex: a TMS-EEG study. J Neurophysiol 2013;109:89–98.
[25] Premoli I, Rivolta D, Espenhahn S, Castellanos N, Belardinelli P, Ziemann U, et al. Characterization of GABAB-receptor mediated neurotransmission in the human cortex by paired-pulse TMS–EEG. Neuroimage 2014;103:152–62.
[26] Oldfield RC. The assessment and analysis of handedness: the Edinburgh inventory. Neuropsychologia 1971;9:97–113.
[27] Rogasch NC, Thomson RH, Farzan F, Fitzgibbon BM, Bailey NW, Hernandez-Pavon JC, et al. Removing artefacts from TMS-EEG recordings using independent component analysis: importance for assessing prefrontal and motor cortex network properties. Neuroimage 2014;101:425–39.
[28] Delorme A, Makeig S. EEGLAB: an open source toolbox for analysis of single-trial EEG dynamics including independent component analysis. J Neurosci Methods 2004;134:9–21.
[29] Oostenveld R, Fries P, Maris E, Schoffelen J-M. FieldTrip: open source software for advanced analysis of MEG, EEG, and invasive electrophysiological data. Comput Intell Neurosci 2010; <http://dx.doi.org/10.1155/2011/156869>.
[30] Hyvärinen A, Oja E. Independent component analysis: algorithms and applications. Neural Netw 2000;13:411–30.
[31] Rogasch NC, Daskalakis ZJ, Fitzgerald PB. Cortical inhibition of distinct mechanisms in the dorsolateral prefrontal cortex is related to working memory performance: a TMS–EEG study. Cortex 2015;64:68–77.
[32] Komssi S, Kähkönen S, Ilmoniemi RJ. The effect of stimulus intensity on brain responses evoked by transcranial magnetic stimulation. Hum Brain Mapp 2004;21:154–64.
[33] Dunn OJ. Multiple comparisons using rank sums. Technometrics 1964;6:241–52.
[34] Maris E, Oostenveld R. Nonparametric statistical testing of EEG-and MEG-data. J Neurosci Methods 2007;164:177–90.
[35] Cash RFH, Ziemann U, Murray K, Thickbroom GW. Late cortical disinhibition in human motor cortex: a triple-pulse transcranial magnetic stimulation study. J Neurophysiol 2010;103:511–18.
[36] Nakamura H, Kitagawa H, Kawaguchi Y, Tsuji H. Intracortical facilitation and inhibition after transcranial magnetic stimulation in conscious humans. J Physiol (Lond) 1997;498:817–23.
[37] Di Lazzaro V, Oliviero A, Mazzone P, Pilato F, Saturno E, Insola A, et al. Direct demonstration of long latency cortico-cortical inhibition in normal subjects and in a patient with vascular parkinsonism. Clin Neurophysiol 2002;113:1673–9.
[38] Müller-Dahlhaus JFM, Liu Y, Ziemann U. Inhibitory circuits and the nature of their interactions in the human motor cortex – a pharmacological TMS study. J Physiol (Lond) 2008;586:495–514.

[39] Fitzgerald PB, Maller JJ, Hoy K, Farzan F, Daskalakis ZJ. GABA and cortical inhibition in motor and non-motor regions using combined TMS–EEG: a time analysis. Clin Neurophysiol 2009;120:1706–10.
[40] Fitzgerald PB, Daskalakis ZJ, Hoy K, Farzan F, Upton DJ, Cooper NR, et al. Cortical inhibition in motor and non-motor regions: a combined TMS-EEG study. Clin EEG Neurosci 2008;39:112–17.
[41] Farzan F, Barr MS, Levinson AJ, Chen R, Wong W, Fitzgerald PB, et al. Reliability of long-interval cortical inhibition in healthy human subjects: a TMS–EEG study. J Neurophysiol 2010;104:1339–46.
[42] Premoli I, Castellanos N, Rivolta D, Belardinelli P, Bajo R, Zipser C, et al. TMS-EEG signatures of GABAergic neurotransmission in the human cortex. J Neurosci 2014;34:5603–12.
[43] Mäki H, Ilmoniemi RJ. The relationship between peripheral and early cortical activation induced by transcranial magnetic stimulation. Neurosci Lett 2010;478:24–8.
[44] Devanne H, Lavoie BA, Capaday C. Input-output properties and gain changes in the human corticospinal pathway. Exp Brain Res 1997;114:329–38.
[45] Ferbert A, Priori A, Rothwell J, Day B, Colebatch J, Marsden C. Interhemispheric inhibition of the human motor cortex. J Physiol (Lond) 1992;453:525–46.
[46] Chen R, Yung D, Li J-Y. Organization of ipsilateral excitatory and inhibitory pathways in the human motor cortex. J Neurophysiol 2003;89:1256–64.
[47] Ni Z, Gunraj C, Nelson AJ, Yeh I-J, Castillo G, Hoque T, et al. Two phases of interhemispheric inhibition between motor related cortical areas and the primary motor cortex in human. Cereb Cortex 2009;19:1654–65.
[48] Daskalakis ZJ, Christensen BK, Fitzgerald PB, Roshan L, Chen R. The mechanisms of interhemispheric inhibition in the human motor cortex. J Physiol (Lond) 2002;543:317–26.
[49] Benarroch EE. GABA(B) receptors: structure, functions, and clinical implications. Neurology 2012;78:578–84.
[50] Nikouline V, Ruohonen J, Ilmoniemi RJ. The role of the coil click in TMS assessed with simultaneous EEG. Clin Neurophysiol 1999;110:1325–8.
[51] Tiitinen H, Virtanen J, Ilmoniemi RJ, Kamppuri J, Ollikainen M, Ruohonen J, et al. Separation of contamination caused by coil clicks from responses elicited by transcranial magnetic stimulation. Clin Neurophysiol 1999;110:982–5.
[52] ter Braack EM, de Vos CC, van Putten MJ. Masking the auditory evoked potential in TMS–EEG: a comparison of various methods. Brain Topogr 2015;28:520–8.
[53] Julkunen P, Säisänen L, Könönen M, Vanninen R, Kälviäinen R, Mervaala E. TMS-EEG reveals impaired intracortical interactions and coherence in Unverricht-Lundborg type progressive myoclonus epilepsy (EPM1). Epilepsy Res 2013;106:103–12.